



Published in final edited form as:

Chem Mater. 2009 October 13; 21(19): 4608–4613. doi:10.1021/cm901666b.

Fabrication of Silica Shell Photonic Crystals through Flexible Core Templates

Luling Wang and Sanford A. Asher*

Department of Chemistry, University of Pittsburgh, Pittsburgh, Pennsylvania 15260

Abstract

We attached very small silica particles onto flexible monodisperse poly (*N*-isopropylacrylamide, PNIPAm) core particles synthesized by dispersion polymerization. These silica particles were attached to the partially swollen PNIPAm particles by the hydrolysis and condensation of tetraethoxysilane at 24 °C. The resulting silica particle-functionalized PNIPAm core particles show reversible swelling and shrinking as the temperature is cycled. These particles form close-packed-array photonic crystals as the solvent evaporates; the cores shrink to form a silica shell around the pure PNIPAm dry core particles as they close pack. The PNIPAm cores were removed by calcination, leaving a PC composed of essentially pure continuous silica shells. These silica shell photonic crystals Bragg diffract UV light at ~310 nm. The close packed particle interstices are continuous and are easily filled by water. In contrast, the silica shells are impervious to water because the process of making them results in a continuous shell of silica without holes.

Keywords

Poly (*N*-isopropylacrylamide); Core-Shell particles; Silica; Sol-gel process; Photonic crystals

1. Introduction

Developing synthetic methodologies to fabricate monodisperse nano and mesoscale materials is important because these materials can be used as the building blocks for novel complex and smart materials such as catalysts,¹ drug delivery materials² and photonic crystals (PCs).³⁻¹³ It would be especially useful if these building blocks could self assemble into functional devices.⁵⁻⁸

PC materials are of great technological interest because they can be used to control the propagation of light, for example, in future photonic circuitry.¹⁴⁻¹⁶ In the simplest cases PCs will possess one dimensional periodicities which will result in photonic bandgaps for specific spectral intervals at specific angles that meet the Bragg condition.⁵⁻⁸ Light at wavelengths and angles that meet the Bragg diffraction condition cannot propagate through PC materials. The PC diffraction efficiencies, the diffraction wavelengths and the diffraction bandwidths depend upon the periodicity of the PC refractive index modulation and the modulation depth.^{16, 17}

Much of the work in photonic crystals has utilized materials made from colloidal particles. In this case the important parameters include the particle refractive index, its diameter and the particle morphology.¹⁸⁻²¹ Some particle array crystal structures, such as the inverse face centered cubic (fcc) structure permit the PC to possess 3-D photonic bandgaps if a sufficiently

* Corresponding author asher@pitt.edu. Phone: 412-624-8570. Fax: 412-624-0588. luw2@pitt.edu.

large refractive index contrast occurs between the sphere air holes and the interstitial spaces.²²⁻²⁵

There is an extensive literature describing methods to synthesize the simplest monodisperse building blocks of PC, which are colloidal spheres of specific size possessing particular surface functionalities.²⁶⁻²⁹ These monodisperse colloidal particles can be composed of polymer²⁸ or inorganic²⁹ or metallic materials.³⁰ In addition, more complex spherical colloidal particles have been synthesized which contain nanoscopic inclusions such as semiconductor quantum dots, as well as silver, gold and other quantum dots.^{6, 31, 32} These particles can form close-packed PCs through various methods of packing such as slow sedimentation and solvent evaporation,³³ centrifugation,³⁴ spin coating³⁵ and convective self-assembly.³⁶

Alternatively, charged colloidal particles have been synthesized whose surfaces are functionalized by strong acid groups.⁵⁻⁸ These charged particles in pure water readily self assemble into highly ordered crystalline colloidal arrays (CCA) PCs.⁵⁻⁸

The next level of complexity for colloidal particle building blocks would utilize additional design degree of freedoms enabled by the use of particles which consist only of hollow spherical shells.^{5, 18-21} The diffraction properties could be controlled by modifying the colloidal particle shell thickness, as well as by controlling the refractive index of materials which are diffused into the cores of the hollow spherical shells.^{19-21, 37} In addition, the shell material could be replaced by air to form air shell complex PC structures.

We have been working on developing PC composed of shells of colloidal particles. We were among the first to synthesize monodisperse hollow spherical polystyrene shell particles and were the first to form PCs from hollow particles.⁵ We prepared monodisperse core-shell particles by polymerizing a polystyrene shell around a silica core. Etching away the silica core resulted in hollow monodisperse polystyrene particles. A major limitation was that the polystyrene shell was flexible like a balloon and could collapse to form bowl shaped structures. Other synthetic approaches have fabricated more structurally rigid shells out of silica and titania etc.^{18, 38-47}

Caruso et al.³⁸⁻⁴⁰ utilized a layer-by-layer self-assembly technique to coat submicron spherical polymer particles with silica nanoparticles. The polymer core was then removed by dissolution or calcination to create hollow particles. Hollow silica spheres were also synthesized through the hydrolysis and condensation of tetraethoxysilane (TEOS) on the surface of polystyrene particles⁴¹ or on ZnS particles.⁴² The core was then removed to produce hollow spherical silica shells. Wong et al.⁴³ reported a room-temperature, wet chemical-based synthesis route in which silica and gold nanoparticles were cooperatively assembled with lysine-cysteine diblock copolypeptides into robust hollow spheres. Chen et al.^{44, 45} reported a technique to fabricate hollow silica shells and hollow titania shells via a one-step process where the polystyrene core particles dissolved as the silica shell condensed. Yin et al.⁴⁶ reported the spontaneous transformation of silica colloids from solid particles to hollow spheres in the presence of NaBH_4 .

In addition, Colvin et al.¹⁸ reported a “lost-wax” method that grew colloidal particle shells within an inverse opal template. Xia et al.⁴⁷ prepared mesoscale hollow spheres of TiO_2 and SnO_2 by templating their sol-gel condensation products within a crystalline array of monodisperse polystyrene particles.

Small ~30 nm hollow spherical rigid shells have been synthesized by using of polymeric micelles.⁴⁸ The advantages of flexible micelles or microgels are that the size and morphology of the particles can be easily tuned by adjusting the solution temperature, ionic strength and solvent composition.⁴⁹

In the work here we demonstrate the synthesis of monodisperse silica shells around a flexible PNIPAm colloidal particle core. We first attach very small silica particles onto the exterior of swollen PNIPAm particles. PNIPAm is a well-known polymer that is highly swollen in water below its lower critical solution temperature (LCST). Above this temperature it undergoes a reversible volume phase transition to a collapsed, dehydrated state.⁷ The swollen PNIPAm core particles are utilized as a highly elastic and soft template. As solvent is evaporated from a dispersion of these monodisperse core-shell particles the PNIPAm cores shrink and the silica particles on the surface form a silica shell. During this process the core-shell particles self assemble into a close-packed array PC. The system is further condensed as the core is removed by calcination at high temperature.

2. Experimental Section

Preparation of monodisperse PNIPAm core particles

PNIPAm nanoparticles were synthesized by dispersion polymerization. 1.4 g NIPAm, 2.0 g polyvinylpyrrolidone (PVP40), 0.066 g N,N'-methylenebisacrylamide (BIS) were dissolved in 95 mL water and bubbled with nitrogen gas for 0.5 hr. 0.2 g α , α' -azodiisobutyramidine dihydrochloride (AIBA, initiator, Fluka) was dissolved in 5 mL water and bubbled with nitrogen gas before addition. The polymerization was carried out at 70 °C for 6 hr under a nitrogen atmosphere and then the reaction mixture was cooled to room temperature while stirring. The particle solution was filtered through glass wool and dialyzed for 14 days by using 10,000 MWCO dialysis tubing (Pierce). Water was changed three times a day. The particles were characterized by both transmission electron microscopy (TEM) and dynamic light scattering (DLS).

Preparation of PNIPAm-silica core-shell particles

The silica coating process was carried out by hydrolysis and condensation of TEOS on the surface of the PNIPAm nanoparticles by using either of two different recipes. In the first example, 1.0 mL of a PNIPAm (0.80 wt %) particle dispersion was added to 9 mL water under stirring. The mixture was adjusted to pH 11.0 with ammonium hydroxide. 30 μ L TEOS was added to the solution under stirring. The reaction was continued for 4 hr at 24 °C and the resulting particles were characterized by TEM. The second recipe was the same except that the pH was initially adjusted to 8.0 with ammonium hydroxide. The temperature dependence of the core-shell particle was characterized by DLS.

Fabrication of silica shell PC

The PNIPAm-silica core-shell particle dispersion was dried overnight at 90 °C to form a close packed PC. Then the sample was heated at 250 °C for 4 hr and at 450 °C overnight to remove the PNIPAm core. The samples were redispersed in water and then characterized by scanning electron microscopy (SEM) and TEM. The reflectance spectrum was taken on microspectrophotometer (Craic Technologies, Inc, QDI 2010). The microscope objective was a Davin reflecting objective 15 \times , NA 0.28.

Characterization

For TEM measurements, a few drops of a dilute dispersion of the nanoparticles were dried on a carbon-coated copper grid (Ted Pella, Inc.) and observed by Philips Mogagni 268 TEM. Samples for SEM were sputter-coated with palladium. SEM studies were performed on Phillips FEG XL-30 FESEM. DLS was measured by using a Brookhaven Corp. ZetaPALS.

3. Results and Discussion

Our objective in this work was to synthesize a silica shell close packed PC. To accomplish this we needed to form a flexible silica precursor shell which would survive the ultimate removal of the core. To accomplish this we developed a synthesis of a flexible PNIPAm nanogel core which during the silica condensation was swollen where silica particles attached to the exterior hydrogel surface. We expected that as the system self assembled into the final close packed array the PNIPAm particles would shrink to assemble a fully dense silica shell.

The route for the fabrication of silica shell photonic crystals is shown in Scheme 1. Monodisperse PNIPAm colloidal particles were synthesized by dispersion polymerization. These PNIPAm colloidal particles were then coated with a silica shell. The resulting monodisperse PNIPAm-silica core-shell particles self-assembled into a close-packed PC as the solvent evaporated. Heating decomposed and vaporized the PNIPAm cores, leaving a PC composed of a close-packed array of silica shells that diffracted light.

We originally tried to utilize the negatively charged, monodisperse PNIPAm nanoparticles we previously synthesized^{7, 8} which readily self-assemble into CCA. However, we were unable to fabricate a silica shell on the surface of these PNIPAm particles, presumably because the silica particles are also negatively charged through the ionization of surface silanol groups.

Thus, we instead synthesized positively charged PNIPAm core particles by using the cationic initiator AIBA. In addition, we used the amphiphilic polymer PVP40 instead of anionic sodium dodecyl sulfate (SDS) as a stabilizer during the polymerization. The polymerization process is similar to that described elsewhere.^{44, 50} Figure 1a shows a TEM image of the monodisperse PNIPAm core particles with diameters measured by TEM and DLS of 294 ± 25 nm and 453 ± 4 nm (at 24 °C). The TEM particle size is much smaller than that from DLS due to shrinkage during the drying process. Bragg diffraction iridescence was observed when the particles were centrifuged at 12000 g for 1 hr at 24 °C (Figure 1b).

Figure 2 shows that the diameter of the PNIPAm core colloids decreases from ~512 nm at 10 °C to ~244 nm at 40 °C due to the well known volume phase transition which shows a LCST⁴⁹ of ~32 °C. The turbidity of a dilute unordered dispersion of the PNIPAm core colloids increases as the diameter decreases due to the increased refractive index of the smaller particles.
7

To coat the PNIPAm with silica we utilized a modified Stöber process. A typical reaction mixture contained TEOS as the silica precursor, ammonium hydroxide as the catalyst and water as the reaction solvent. The silica coatings were performed either at pH 11.0 or pH 8.0. Figure 3a shows that at pH 11.0 the PNIPAm core particles were coated with small 20~40 nm silica particles. In addition, other silica aggregates (as indicated by the arrow) and free silica particles (within the rectangle) also form in solution. Figure 3b shows that by slowing the hydrolysis rate by decreasing the pH to 8.0 we obtain monodisperse PNIPAm-silica core-shell particles with a diameter of 456 ± 24 nm and a silica shell thickness of ~80 nm. Iridescence of this sample was also observed (similar to Figure 1b) after centrifugation.

Figure 4 shows the temperature dependence of apparent diameter of the PNIPAm-silica core-shell particles. After silica coating the particle has a diameter of 520 ± 3 nm (at 24 °C) which is about 70 nm larger than that of original PNIPAm core particles at 24 °C (453 ± 4 nm). As the temperature increases to 40 °C, the core-shell particle diameter decreases to 280 ± 4 nm. This diameter is also about 40 nm larger than that of the PNIPAm core particles (244 ± 2 nm at 40 °C). After heating to 40 °C during the first temperature cycle, the core-shell particle diameter does not fully return to its original diameter; at 24 °C it has a 28 % decreased diameter of 374 ± 3 nm. The silica shell prevents the full expansion of the core-shell particle. Further

temperature cycles show continued reversible expansions and contractions of this core shell particle.

Figure 5a shows SEM of 210 nm diameter unordered PNIPAm-silica core-shell particles formed by slow sedimentation followed by drying in air. By carefully controlling the temperature and slowly evaporating water,³³ we fabricated an ordered, close-packed structure as shown in Figure 5b. If the image of the particles is magnified, numerous small white dots appear which derive from the silica particles on the surface of the PNIPAm cores.

Figure 6a shows SEM of the ordered hollow close packed silica shell structure formed after removal of the polymer core by calcination. Ordered hollow silica structures can be clearly observed. Figure 6b shows a TEM of a very thin evaporated sample where the individual silica shells can be discerned. The diameter of the hollow core measured by both TEM and SEM is ~140 nm. This diameter is much less than that measured for the pure shrunken PNIPAm particles, presumably because the silica shell further collapses upon calcination. We measure a ~15 nm shell thickness by using TEM and SEM.

Figure 7 shows the reflectance spectrum of these close-packed silica shell PCs measured at normal incidence by using a microspectrophotometer. The reflectance peaks in Figure 7 result from Bragg diffraction from the ordered structure⁵¹ of the silica shell PCs. We assume that the silica shells arrange in an ideal fcc close-packed array where the volume fraction composed of the silica shells and hollow cores is 0.74. This leaves the interstitial space volume fraction to be 0.26.

We measured the diffraction for the dried PC as well as for the same PC immersed in water. We expected a large diffraction red shift due to the increase in refractive index due to the expected increase in water volume fraction. In contrast, Figure 7 shows little shift of the diffraction peak wavelength between air (~306 nm) and water (~321 nm) which indicates only a ~5 % increase in refractive index. Apparently, water cannot penetrate to the cores.

We calculated the impact of water only filling the interstices from equations 1-3, where n_{avg} is the average refractive index of the PC which relates the wavelength diffracted, λ to the lattice spacing, d and glancing angle, θ in Bragg's law: $\lambda = 2 n_{avg} d \sin\theta$. Eqn. 1 calculates n_{avg} assuming that water can only fill the interstices but not the cores. The volume fraction of interstices for close packed spherical particles is 0.26. n_w , n_{SiO_2} and n_{air} are the refractive indices of the solvent, silica (1.425) and air (1.000), ϕ_{SiO_2} is the volume fraction of silica shells, D is the outside diameter of the core-shell particles and D_i is the diameter of the hollow cores.

$$n_{ave} = 0.26n_w + n_{SiO_2} \phi_{SiO_2} + (0.74 - \phi_{SiO_2})n_{air} \quad (1)$$

$$\phi_{SiO_2} = \frac{D^3 - D_i^3}{D^3} \cdot 0.74 \quad (2)$$

$$\lambda = 2 \left(\frac{2}{3} \right)^{\frac{1}{2}} D \cdot n_{ave} \quad (3)$$

We calculate $n_{\text{avg}} = 1.139$ in air and $n_{\text{avg}} = 1.224$ in water. Thus, we calculate that we will observe a red shift of $\sim 7\%$, close to that experimentally observed. This indicates that the cores are actually sealed during the calcination process.

4. Conclusions

We developed a synthesis to attach silica particles onto flexible monodisperse PNIPAm nanogel core particles. These PNIPAm-silica core-shell particles show reversible swelling and shrinking in water as the temperature is cycled. Slow evaporation of solvent causes these particles to self assemble into a close packed PC. Calcination removes the PNIPAm particle core leaving a PC composed of a silica shell close packed array which has air both in the interstices as well as in the cores. The shrinking of the silica shell/PNIPAm core particles during solvent evaporation and calcination seals the cores due to formation of a continuous silica shell. This makes the shells impermeable to water.

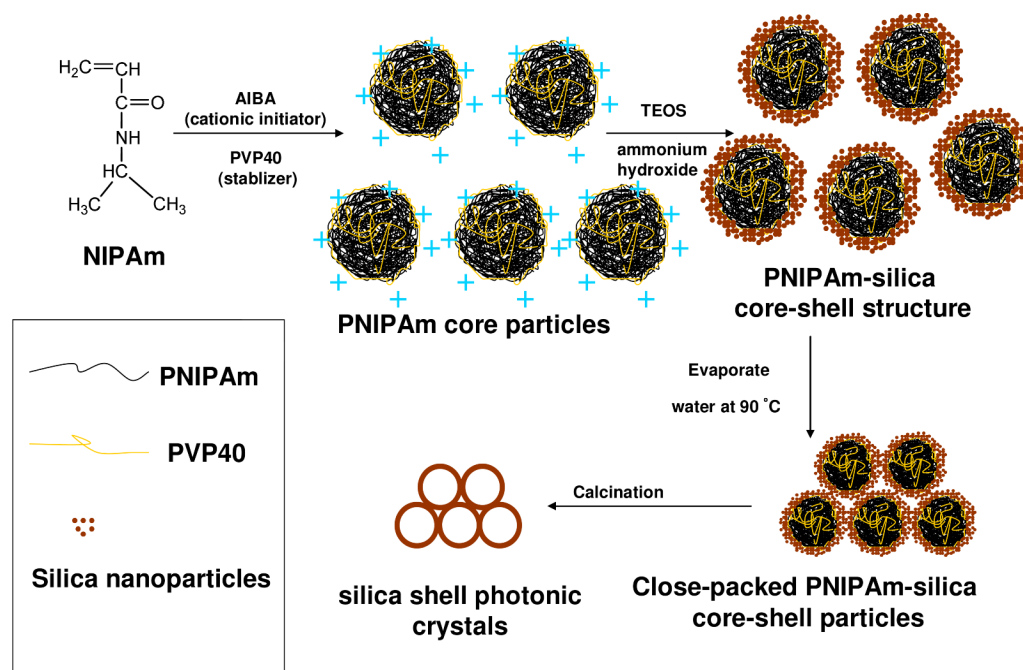
Acknowledgments

The authors acknowledge support for this work from the National Institutes of Health NIH (NIBIB) grant 1R01EB009089. The authors also thank Dr. Sasha Tikhonov, Jia Luo and Justin Bohn for many helpful discussions.

References

1. Bell AT. *Science* 2003;299:1688. [PubMed: 12637733]
2. Lai C, Trewyn BG, Jeftinija DM, Jeftinija K, Xu S, Jeftinija S, Lin V. *J. Am. Chem. Soc* 2003;125:4451. [PubMed: 12683815]
3. Chang S, Liu L, Asher SA. *J. Am. Chem. Soc* 1994;116:6739.
4. Chang S, Liu L, Asher SA. *J. Am. Chem. Soc* 1994;116:6745.
5. Xu X, Asher SA. *J. Am. Chem. Soc* 2004;126:7940. [PubMed: 15212543]
6. Wang W, Asher SA. *J. Am. Chem. Soc* 2001;123:12528. [PubMed: 11741416]
7. Weissman JM, Sunkara HB, Tse AS, Asher SA. *Science* 1996;274:959. [PubMed: 8875932]
8. Reese CE, Mikhonin AV, Kamenjicki M, Tikhonov A, Asher SA. *J. Am. Chem. Soc* 2004;126:1493. [PubMed: 14759207]
9. Nayak S, Lyon LA. *Angew. Chem. Int. Ed* 2005;44:7686.
10. Lyon LA, Debord JD, Debord SB, Jones CD, McGrath JG, Serpe M. *J. Phys. Chem. B* 2004;108:19099.
11. Suzuki D, McGrath JG, Kawaguchi H, Lyon LA. *J. Phys. Chem. C* 2007;111:5667.
12. Gorelikov I, Field LM, Kumacheva E. *J. Am. Chem. Soc* 2004;126:15938. [PubMed: 15584708]
13. Suzuki D, Kawaguchi H. *Langmuir* 2005;21:8175. [PubMed: 16114919]
14. Yablonovitch E. *Phys. Rev. Lett* 1987;58:2059. [PubMed: 10034639]
15. John S. *Phys. Rev. Lett* 1987;58:2486. [PubMed: 10034761]
16. Joannopoulos, JD.; Johnson, SG.; Winn, JN.; Meade, RD. *Photonic crystals: Molding the Flow of the Light*. Second Edition. Princeton University; New Jersey: 2008.
17. Joannopoulos JD, Villeneuve PR, Fan SH. *Nature* 1997;387:830.
18. Jiang P, Bertone JF, Colvin VL. *Science* 2001;291:453. [PubMed: 11161193]
19. Colvin VL. *MRS Bull* 2001;26:637.
20. Rengarajan R, Jiang P, Colvin V, Mittleman D. *Appl. Phys. Lett* 2000;77:3517.
21. Busch K, John S. *Phys. Rev. E* 1998;58:3896.
22. Norris DJ, Vlasov YA. *Adv. Mater* 2001;13:371.
23. Miguez H, Meseguer F, Lopez C, Lopez-Tejiera F, Sanchez-Dehesa J. *Adv. Mater* 2001;13:393.
24. Blanco A, Chomski E, Grabtchak S, Ibsate M, John S, Leonard SW, Lopez C, Meseguer F, Miguez H, Mondia JP, Ozin GA, Toader O, van Driel HM. *Nature* 2000;405:437. [PubMed: 10839534]

25. Zakhidov AA, Baughman RH, Iqbal Z, Cui C, Khayrullin I, Dantas SO, Marti J, Ralchenko VG. *Science* 1998;282:897. [PubMed: 9794752]
26. Stöber W, Fink A. *J. Colloid Interface Sci* 1968;26:62.
27. Krieger IM, O'Neill FM. *J. Am. Chem. Soc* 1968;90:3114.
28. Reese CE, Guerrero CD, Weissman JM, Lee K, Asher SA. *J. Colloid Interface Sci* 2000;232:76. [PubMed: 11071735]
29. Eshuis A, Koning CAJ. *Colloid Polym. Sci* 1994;272:1240.
30. Graf C, van Blaaderen A. *Langmuir* 2002;18:524.
31. Murray CB, Norris DJ, Bawendi MG. *J. Am. Chem. Soc* 1993;115:8706.
32. Jones CD, Lyon LA. *J. Am. Chem. Soc* 2003;125:460. [PubMed: 12517159]
33. Miguez H, Meseguer F, Lopez C, Mifsud A, Moya JS, Vazquez L. *Langmuir* 1997;13:6009.
34. Holland BT, Blanford CF, Do T, Stein A. *Chem. Mater* 1999;11:795.
35. Mihi A, Ocana M, Miguez H. *Adv. Mater* 2006;18:2244.
36. Norris DJ, Arlinghaus EG, Meng L, Heiny R, Scriven LE. *Adv. Mater* 2004;16:1393.
37. Blanford CF, Schroden RC, Al-Daous M, Stein A. *Adv. Mater* 2001;13:26.
38. Caruso RA, Susha A, Caruso F. *Chem. Mater* 2001;13:400.
39. Caruso F, Caruso RA, Mohwald H. *Chem. Mater* 1999;11:3309.
40. Caruso F, Caruso RA, Mohwald H. *Science* 1998;282:1111. [PubMed: 9804547]
41. Tissot I, Reymond JP, Lefebvre F, Bourgeat-Lami E. *Chem. Mater* 2002;14:1325.
42. Velikov KP, van Blaaderen A. *Langmuir* 2001;17:4779.
43. Wong MS, Cha JN, Choi K, Deming TJ, Stucky GD. *Nano Lett* 2002;2:583.
44. Chen M, Wu L, Zhou S, You B. *Adv. Mater* 2006;18:801.
45. Cheng X, Chen M, Wu L, Gu G. *Langmuir* 2006;22:3858. [PubMed: 16584267]
46. Zhang T, Ge J, Hu Y, Zhang Q, Aloni S, Yin Y. *Angew Chem* 2008;120:5890.
47. Zhong Z, Yin Y, Gates B, Xia Y. *Adv. Mater* 2000;12:206.
48. Khanal A, Inoue Y, Yada M, Nakashima K. *J. Am. Chem. Soc* 2007;129:1534. [PubMed: 17283999]
49. Pelton R. *Adv. Colloid Interface Sci* 2000;85:1. [PubMed: 10696447]
50. Bamnolker H, Nitzan B, Gura S, Margel S. *J. Mater. Sci. Lett* 1997;16:1412.
51. Yu A, Meiser F, Cassagneau T, Caruso F. *Nano Lett* 2004;4:177.



Scheme 1.
Preparation of silica shell photonic crystals

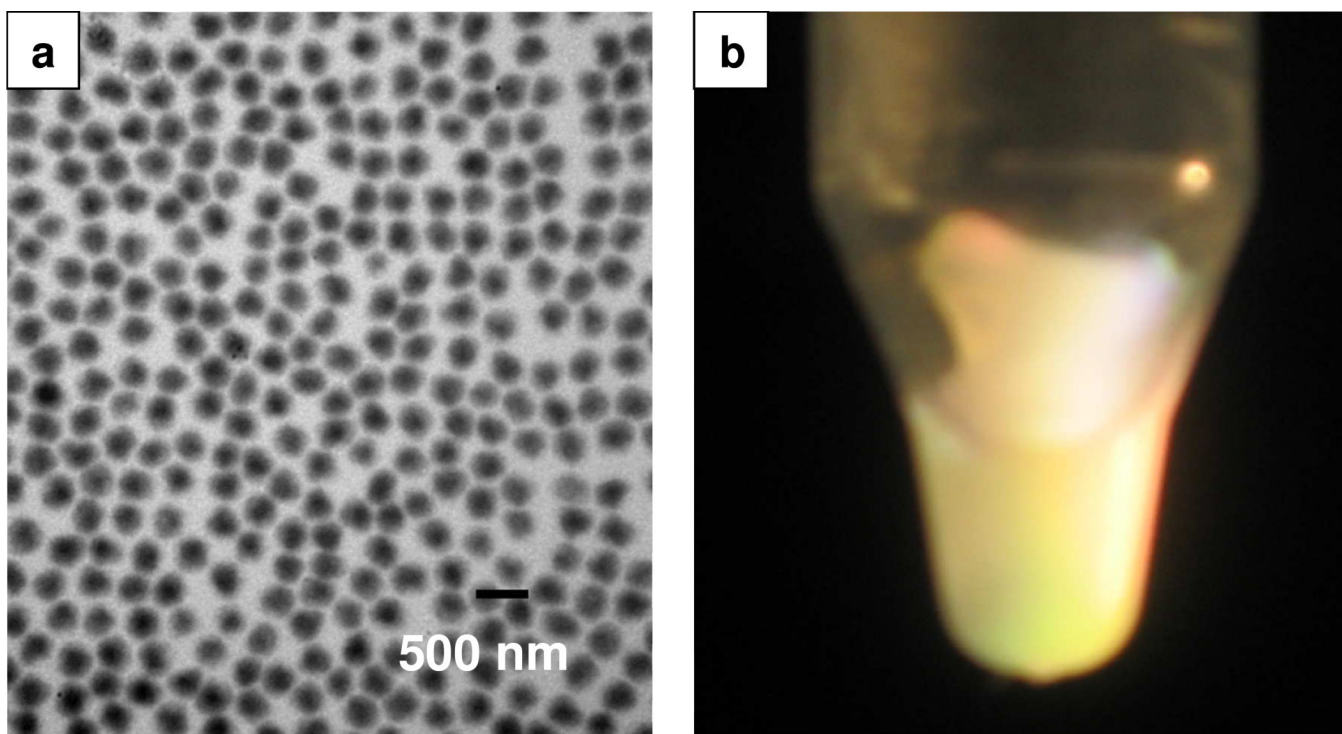


Figure 1.
a) TEM image of PNIPAm core particles; b) Photograph of Bragg diffraction from PNIPAm core particles

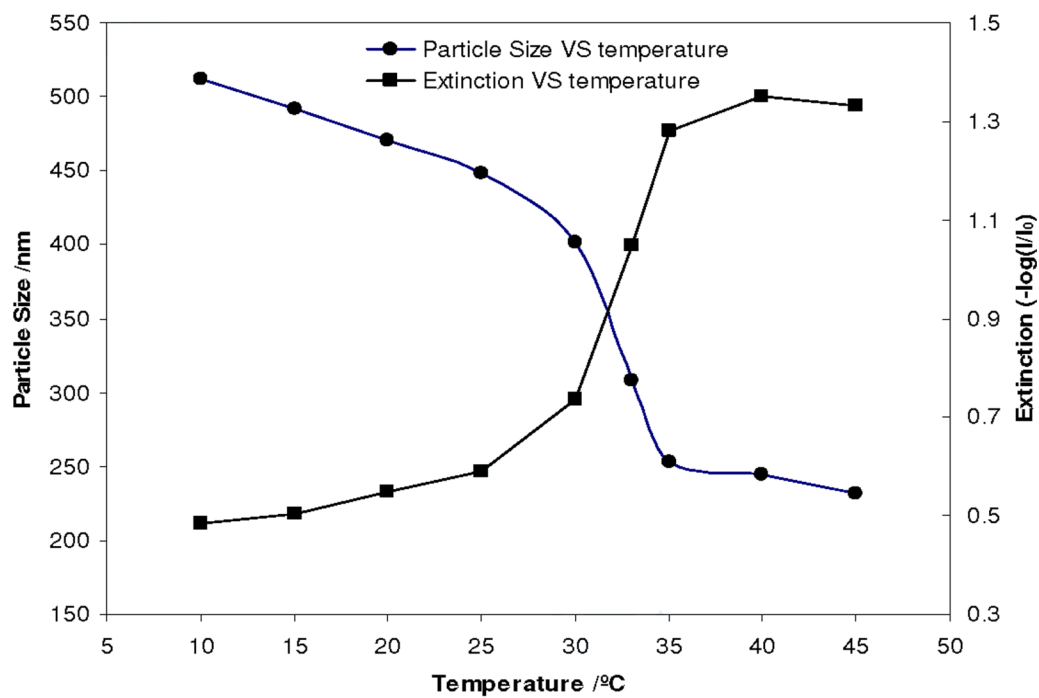


Figure 2. Temperature dependence of diameter and turbidity of PNIPAm particles

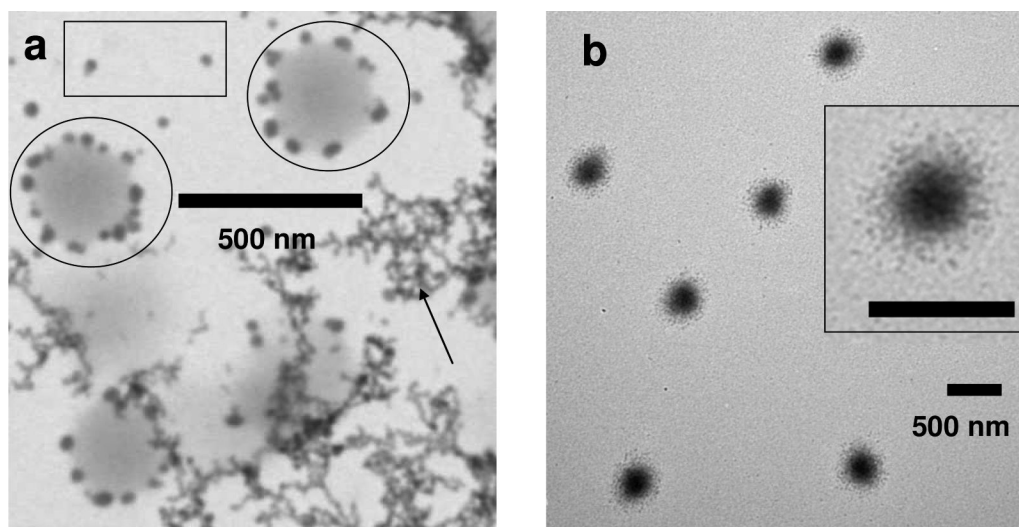


Figure 3. TEM of PNIPAm core particles after silica coating at a), pH 11.0 and b), pH 8.0 (the insert shows a core-shell particle at higher magnification, the scale bar is 500 nm)

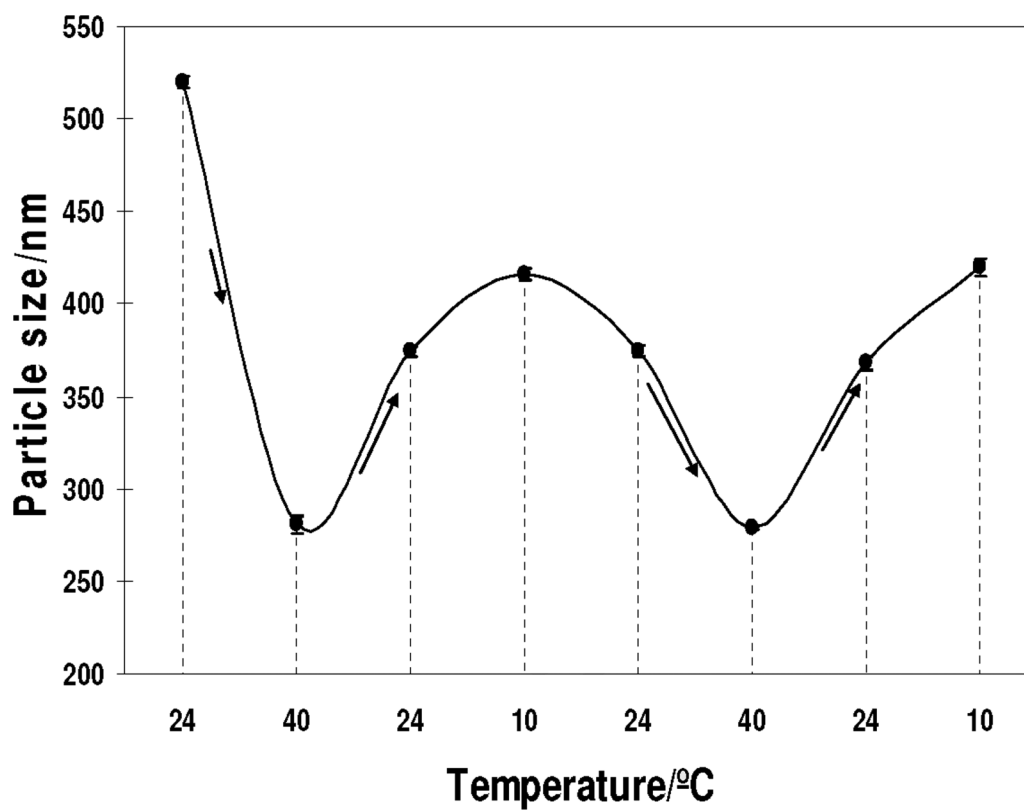


Figure 4. Temperature dependence of the DLS measured apparent particle diameter of the PNIPAm-silica core-shell particles (solid line drawn to help the eye)

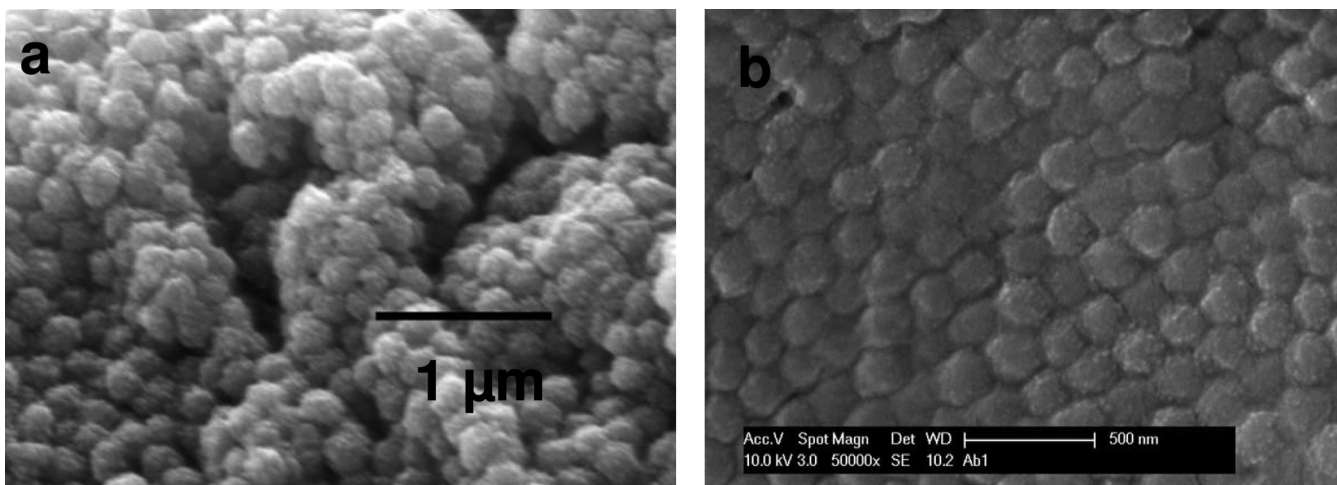


Figure 5.
SEM of (a) unordered and (b) ordered close-packed silica-shell/PNIPAm-core particles

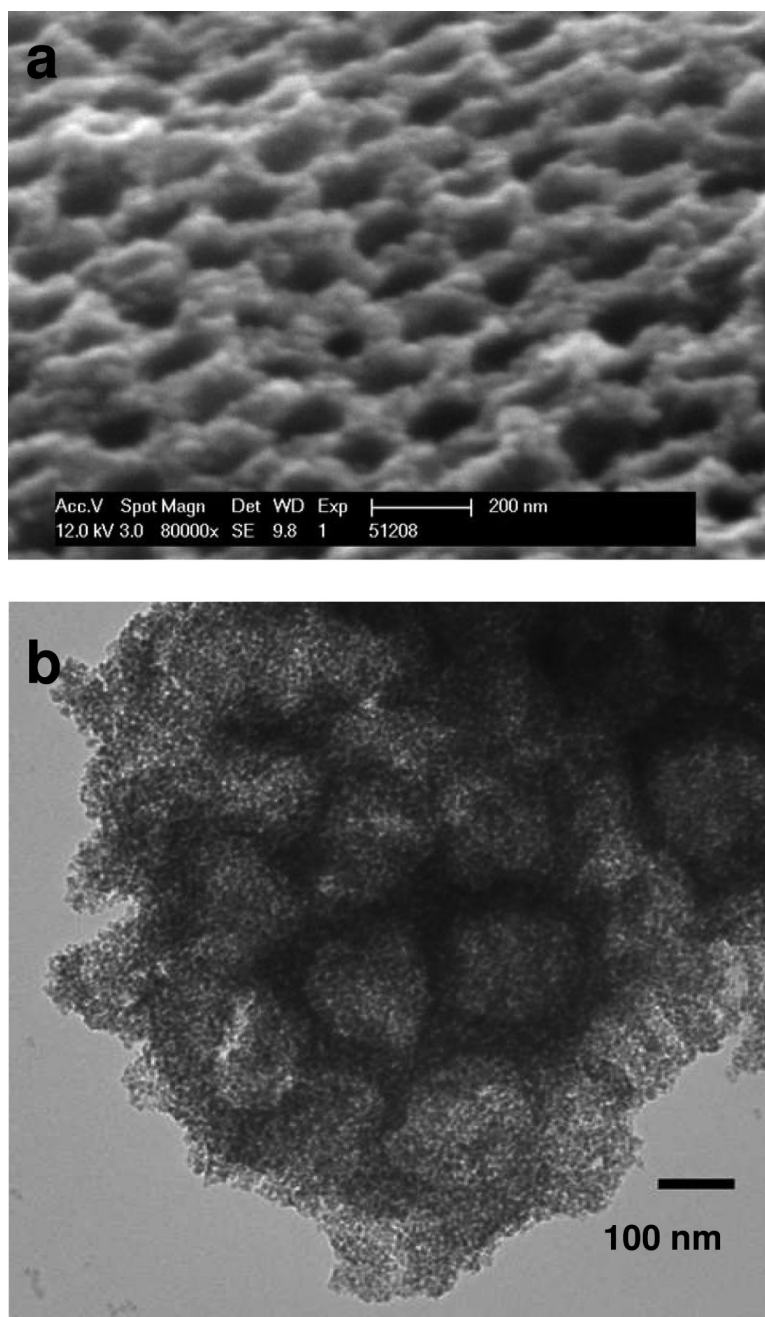


Figure 6. (a) SEM image of the cross section of silica shell photonic crystals, (b) TEM image of the silica shell photonic crystals

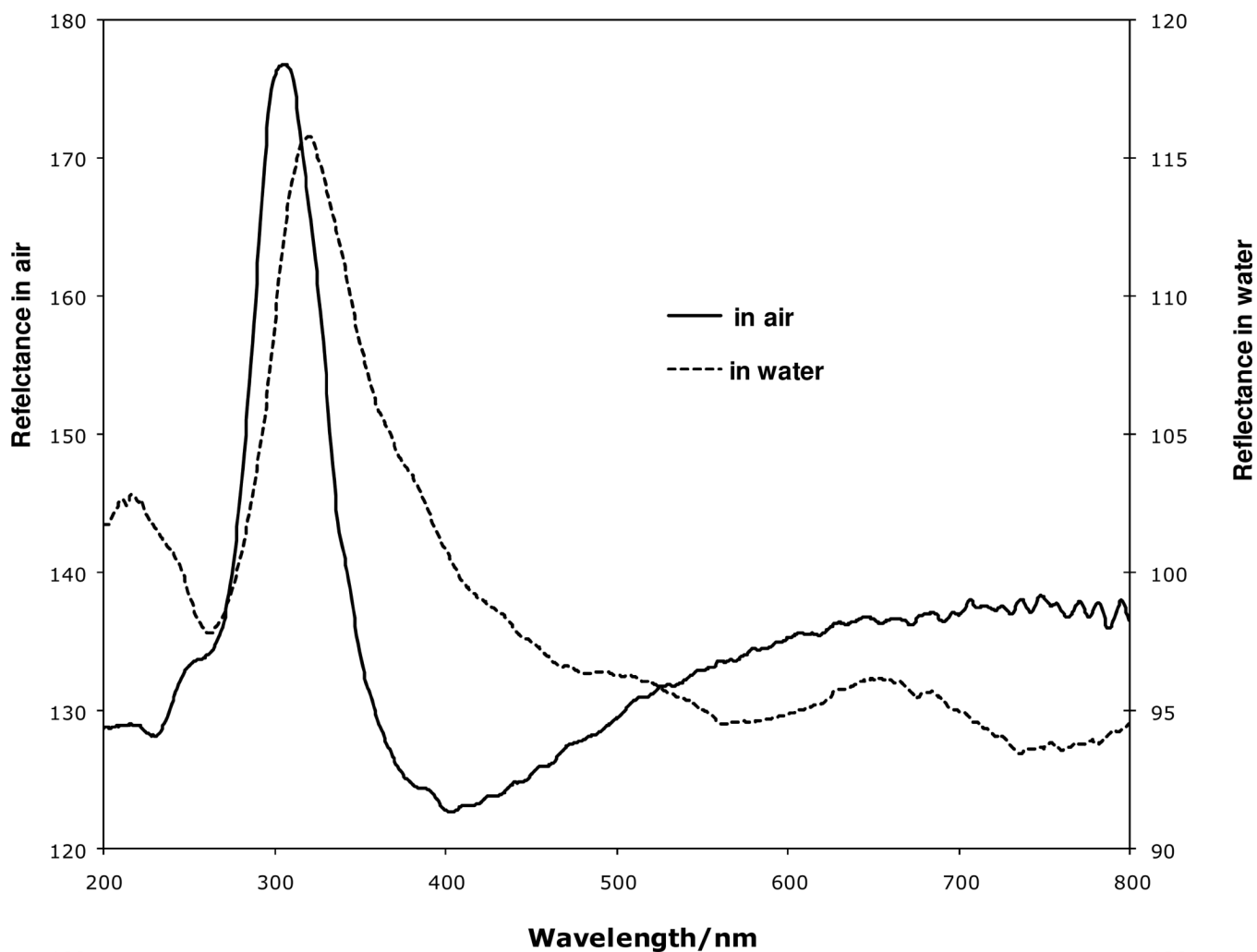


Figure 7. Reflectance spectrum of silica shell photonic crystals in air (solid line) and water (dash line)